

# The birth of defects in pattern formation: Testing of the Kibble–Zurek mechanism

S. Casado<sup>1</sup>, W. González-Viñas<sup>1,a</sup>, S. Boccaletti<sup>2</sup>, P.L. Ramazza<sup>2</sup>, and H. Mancini<sup>1</sup>

<sup>1</sup> Complex Systems Group, Dept. of Phys. and Appl. Math., Universidad de Navarra, Irunlarrea s/n, 31080 Pamplona, Spain

<sup>2</sup> CNR – Istituto dei Sistemi Complessi, via Madonna del Piano 10, 50019 Sesto Fiorentino, Italy

**Abstract.** The extension of the cosmological mechanism of Kibble to second order phase transitions in condensed matter systems by Zurek, can be further generalized to bifurcations of out-of-equilibrium systems in continuum media, since the argument used in the derivation of the Kibble–Zurek scaling law is general. Here we review the validity of such scaling comparing several bifurcations where the test has been checked. Also, new experimental results of a nonlinear optical system are reported.

## 1 Introduction

Defects play an important role in fundamental aspects of Science, as for example their mediation in phase transitions [1–3], and in general where breaking of symmetries are relevant [4–6]. Also defects are very important in the quality of coatings, in materials processing, in semiconductors, in genetics, among many other fields.

From the point of view of physics, a defect could be defined as a localized state which has less symmetries than the linearly stable global state. Thus, the global state has a (locally) broken symmetry due to the existence of the defect. The topological properties of defects can be studied through their homotopy group [7–10].

The symmetries in a system could be inherited in the relevant variables which characterize its state, giving rise to the structures which, when their typical lengths and times are at a human scale, are commonly called patterns. In this case, usually it is possible to define an order parameter to characterize the state in spatial and temporal scales larger than those determined by the equivalent to the wavelength of the state. From the equilibrium phase transitions theory, the order parameter should be zero in the more symmetric phase, while in the less symmetric phase is different of zero. This constraint results in a definition which is useful only in the neighborhood of the transition. Nevertheless, this definition could be extended (in pattern formation) to a range of consecutive symmetry breaking bifurcations, given that the evolution equations consider all the sequence of the symmetries through the transitions, provided that they have the correct coefficients. From this point of view the model equations for the order parameter could describe the dynamics of the system in complex contexts. Also, from the equilibrium phase transitions field it is possible to define a control parameter  $E$  in the system that, if it is changed quasi-statically, the system goes through the possible states, specifically crossing all the bifurcations or transitions considered [11].

There are several mechanisms from which defects appear in patterns. Those mechanisms could be from geometrical constraints where the boundaries make impossible the existence of a perfect pattern, from thermal effects (where defects appear due to the energy given by the

---

<sup>a</sup> e-mail: wens@fisica.unav.es

thermal fluctuations), from nonlinear effects (which could entangle non-trivially into states with tendency to generate defects), or from symmetry changing transitions (where defects usually appear as a consequence of the dynamical adjustment of the system to the new, possibly degenerate, stable state).

The appearance of topological defects is closely related to bifurcations between patterns with symmetry breaking [6]. When crossing one of such bifurcations, phase<sup>1</sup> singularities (the so called topological defect) appear as relics of the more symmetric state. Although the origin of the topological defects is of a higher symmetry, they are localized states stabilized by topological constraints, which reduce the symmetry of the defect (even less symmetric than the globally stable state) [4,5].

In a non equilibrium bifurcation the reduced control parameter is defined as

$$\epsilon \equiv \frac{E - E_c}{E_c}, \quad (1)$$

where  $E_c$  is the value of the control parameter at which the stable state before the transition becomes linearly unstable. It is usually considered as the (non-reduced critical) control parameter for the primary bifurcation, i.e. one bifurcation which transitions from a homogeneous state to a patterned one.

In a standard phase transition the most symmetric phase occurs at very high temperatures (the temperature is the main control parameter) because the thermal energy (disordering field) is much greater than the other involved energies (for example, those corresponding to the ordering magnetic field). This is related to the effect that thermal fluctuations have on the order. However, in a non equilibrium bifurcation the control parameter  $\epsilon$  is closely related to how much the system is out of equilibrium. And the equilibrium is of course homogeneous, because if this was not the case, fluxes would appear which would show an out of equilibrium behavior. Thus, the higher the control parameter is, the less symmetries are present in the system. In this case the thermal fluctuations are not relevant and even they might be neglected if the system is not very close to a thermodynamical transition. The important fluctuations are of other origin [12].

Kibble [2] noticed that the early Universe in expansion could imply that different regions of the space-time would be causally uncorrelated through the cosmological phase transitions which actually occurred. In this way, a lack of phase matching could happen between regions due to the falling of the system to different minima coming from the degeneration of the symmetry breaking transition. Thus, phase singularities or topological defects appeared. Those defects in a quickly expanding Universe determined huge energy fluctuations which could be involved in the present distribution of galaxies.

Almost a decade later, Zurek [3,13] noticed that this mechanism is common to all breaking phase transitions. The main difference between a cosmological phase transition, and a condensed matter one is that in the former the limiting speed which define whether two regions are causally non-connected is the speed of light, meanwhile in the latter the limiting speed is much slower and is related more or less to the media (usually the speed of sound). The generalized mechanism is known as the Kibble–Zurek one. It can be summarized in the following way: If the control parameter of the system is changed linearly slowly far from the critical point, the selected state follows adiabatically the control parameter value in such a way that the instantaneous state is the equilibrium one for the instantaneous control parameter. Near a second order transition, the relaxation time which the system goes back to the equilibrium values diverges, in such a way that the system has no time to follow adiabatically the control parameter. So the correlation length, among other magnitudes, should change faster than the limiting speed in the system and consequently gets frozen until the adiabatic dynamics is restored well after the phase transition. The observed correlation length after the critical point is the one the system had when it froze. This kind of mechanism leads to a power law for the correlation length as a function of the rate of change of the control parameter. It is thought that this behavior depends only on the

---

<sup>1</sup> It is worth to say, that here the phase is a fraction of a period in the parameter which defines the degeneracy above. We will use the phase term in both senses along this paper.

space dimension, topology and the dissipative character of the system, therefore constituting a universal scaling law.

Concerning a bifurcation between two out-of-equilibrium states of a system, the Kibble–Zurek mechanism could be extended naturally to report the density of defects of the patterns obtained after a quench in the control parameter. In what follows in this section, we are going to argue this generalization.

Consider either a conserved or not conserved order parameter  $\phi$ , whose evolution equation is:

$$\frac{\partial \phi}{\partial t} = \mathcal{G}[\phi; \epsilon], \quad (2)$$

where the functional  $\mathcal{G}$  could describe either a time-dependent Ginzburg–Landau type equation or a Cahn–Hilliard type equation, among others depending on its form. Consider that  $\epsilon$  is the reduced control parameter, and that the bifurcation is a primary one. The functional  $\mathcal{G}$  can include noise or fluctuations. In that sense the evolution equation is a Stochastic partial differential equation. The original field  $u$  corresponding to the order parameter  $\phi$  can usually be obtained by multiplying the order parameter by the linear modes  $\psi_j$  of the system near the bifurcation. That is, in a system which below the threshold is in the state characterized by  $u_0$ , slightly above the threshold its state could be expressed as:

$$u = u_0 + \sum_j \phi_j \psi_j. \quad (3)$$

Each  $\psi_j$  represents the broken symmetry through the bifurcation along with its degeneracy. Some degeneracies sometimes can be included in the order parameter as a phase or with other kind of artifacts in such a way that the effective components of the order parameter could be drastically reduced into the sum above.

The degeneracy which comes from the symmetry breaking appears (usually) as the continuous parameter which defines the phase involved in the topological defects [10,14].

Let us call  $\epsilon_c$  the critical reduced control parameter and redefine it in order to be equal to zero, that is referring it to the studied bifurcation. Let also the initial value of the control parameter be  $\epsilon_i < 0$ . Let finally the system attain a stationary state, which is corresponding to  $\phi = 0$ , plus the existence of fluctuations which are unstable and consequently disappear after a while. Those fluctuations are characterized by a correlation length  $\xi$  (and survival time  $\tau$ ) depending on the stationary value of  $\epsilon_i$ . The actual value for  $\xi$  depends on the model: in non relativistic mean-field second order transitions we have  $\xi \sim 1/\sqrt{\epsilon}$  [3,13], while in the quantum Ising model we have  $\xi \sim 1/\epsilon$  [15], among many other possibilities. All these cases can be included in a phase transition picture where

$$\xi \sim \epsilon^{-\nu}, \quad (4)$$

where  $\nu$  is the critical exponent corresponding to the correlation length of the order parameter.

Thus, at the initial state, the value for the correlation length will be  $\xi_i = \xi(\epsilon_i)$ . If the characteristic time for fluctuations of size  $\xi_i$  is  $\tau$ , then the mean time which quasi-domains of fluctuations of size  $\xi_i$  survive is  $\tau$ . So, if we have one of such fluctuations and the control parameter is changed in order to cross the bifurcation in less time than  $\tau$ , that quasi-domain will overcome stable.

In a causally extended system (that is non-connected) all possible degeneracies could be present in the fluctuations field, giving rise to uncorrelated domains corresponding to different values of the phase. In this sense, the macroscopic typical length of the system could be, for example, much larger than the correlation length of the order parameter.

Below a symmetry breaking bifurcation, in the absence of fluctuations, the order parameter  $\phi$  is zero, so the presumably small fluctuations  $\delta\phi$  will follow a linearized version of equation (2). Assuming that

$$\delta\phi = \sum B(\lambda, \mathbf{k}) e^{\lambda t + i\mathbf{k}\cdot\mathbf{r}}, \quad (5)$$

if the system is below the threshold, then small fluctuations should decay exponentially in time to zero; therefore  $\Re[\lambda] < 0$ . However, when the system crosses the bifurcation, at least

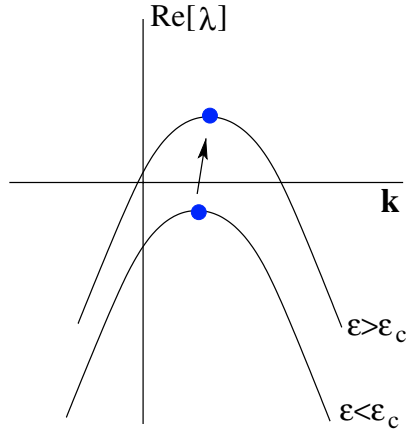


**Fig. 1.** Sketch of the continuity of the modes which show slower decay below the threshold and faster growth above the threshold. Usually these modes have  $\mathbf{k} = 0$ , because the oscillation of the relevant modes is included in  $\psi_j$ .

some components of the fluctuations will grow exponentially in time; therefore  $\Re[\lambda] > 0$ . The evolution characteristic time will be defined through the coefficient of the real exponential  $\exp(\Re[\lambda]t)$ :

$$\tau = \frac{1}{\Re[\lambda]}. \quad (6)$$

It is important to notice that  $\Re[\lambda]$  depends on  $\epsilon$  and  $\mathbf{k}$ , which is the wave vector of the Fourier component for the order parameter, and does not correspond to the linear modes  $\psi_j$ . The fluctuations of the order parameter below the bifurcations are governed by the minimum of the  $|\Re[\lambda]|$ , which gives the highest  $\tau$ , and consequently describe the most durable fluctuations. If the bifurcation is of continuous type (supercritical bifurcation), at the critical point  $\epsilon_c$ , the fluctuations follow  $\Re[\lambda] = 0$ . Thus, in the nearness of  $\epsilon = 0$ :

$$\Re[\lambda] \propto \epsilon g(\epsilon). \quad (7)$$

In general, it is convenient to define the control parameter in such a way that  $g(0)$  is finite but not zero. Then, the so-called slowing down near the critical point of the relevant modes occurs giving:

$$\tau(\epsilon) \sim |\epsilon|^{-1}, \quad (8)$$

that corresponds in the phase transitions theory to a critical exponent  $z\nu = 1$ , where  $z$  is the dynamical critical exponent [16].

On the other side, above the threshold, the relevant fluctuations are those which grow faster and are obtained continuously from those than decay slower below the threshold (figure 1).

If the control parameter  $\epsilon$  is slowly increased through the bifurcation at a constant rate  $\mu$  in such a way that the bifurcation is crossed over at  $t = 0$ , then  $\epsilon(t) = \mu t$ . Assume that  $-t_0$  is the time at which the fluctuations of size  $\xi(\epsilon(-t_0))$  survive  $\tau = 2t_0$ . The size of those fluctuations will be the correlation length (size of domains) selected above the bifurcation. Thus:

$$\epsilon(-t_0) = -\mu t_0 = -\mu\tau/2 \propto -\mu|\epsilon|^{-z\nu}, \quad (9)$$

consequently:

$$|\epsilon(-t_0)|^{1+z\nu} \propto \mu. \quad (10)$$

Then,

$$|\epsilon(\pm t_0)| \propto \mu^{\frac{1}{1+z\nu}}, \quad (11)$$

At  $+t_0$  the dynamics is restored. Therefore, the pattern appears clearly. For almost all the cases,  $z\nu = 1$  and  $\epsilon \sim \sqrt{\mu}$ . To obtain the selected correlation length, it is usual to substitute expression (11) in equation (4); obtaining:

$$|\xi(\pm t_0)| \propto \mu^{-\frac{\nu}{1+z\nu}}. \quad (12)$$

Assuming that the critical exponent of the correlation length is that of a mean field theory ( $\nu = 1/2$ ) then  $|\xi(\pm t_0)| \propto \mu^{-1/4}$ .

It is possible to relate this argument to the following. On one hand, we have:

$$\mu \equiv \frac{d\epsilon}{dt} = \frac{\epsilon|_{t=\tau}}{\tau}, \quad (13)$$

multiplying both sides of the equality by  $\epsilon^{-1-\nu} \propto \frac{d\xi}{d\epsilon} \propto \frac{\xi}{\epsilon}$ . In this way we have that, at the moment of the slowing down:

$$\frac{d\xi}{dt} \sim \frac{\xi}{\tau}. \quad (14)$$

The right side of the equation (14) would be the maximum rate of increase of the correlation length. So, it can be regarded as the limiting speed in the medium. Therefore, the argument given above has a causal nature of Kibble–Zurek type:

$$\frac{d\xi}{dt} \leq v_{\text{lim}} \sim \frac{\xi}{\tau}. \quad (15)$$

Therefore, the system cannot correlate regions non connected in the above sense. Of course, as has been told above, in the case of cosmological transitions (Kibble) the limiting speed is the speed of light, which not depends on  $\mu$ .

Once the correlation length of the fluctuations is frozen, when the dynamics is restored on the basis of the domains determined by that correlation length, there appear a lack of phase matching among the domains which implies the appearance of phase singularities. The mean distance between phase singularities, in the case of zero dimensional defects, will be the correlation length. This fact emphasizes the role of defects in correlating or in decorrelating the structure [17]. Thus, the density of defects  $\rho$  is going to be  $\xi^{-d}$ , where  $d$  the geometrical dimension of the system. As a consequence:

$$\rho \sim \mu^{\frac{d\nu}{1+z\nu}}. \quad (16)$$

In all the experimental cases investigated here  $d = 2$ , and we assume on the base that was told above, that  $z\nu = 1$ , then  $\rho \sim \mu^\nu$ .

Since the establishment of Kibble–Zurek mechanism and its consequences on the confirmation of cosmological theories in a laboratory [13, 18, 19] several experiments have been performed in non-equilibrium phase transitions, among others in liquid crystals [20–22], superfluid helium [23–29], and in superconductors and Josephson junctions [30–35]. Lately some experiments in non-equilibrium bifurcations have also been done in non-linear optical systems [36] and in fluid convection systems [37–39].

In this article we aim at comparing the results of different non-equilibrium bifurcations from the point of view of the Kibble–Zurek mechanism, in order to focus on the peculiarities in this kind of systems. Also, we report new experimental results of the non-linear system studied by Ducci et al. [36] in a new configuration which leads to a different pattern and selection of it. The new experimental results can shed light on why some of the other experiments in non-equilibrium bifurcations which seem not to give the expected scaling exponents.

After this introduction to the subject, the article has been organized in the following way: Firstly, the measurement process and image analysis will be briefly explained. Secondly, we will focus on the conduction-convection bifurcations and their results. Thirdly, we will do the same for the nonlinear optical systems. There, the new experimental results will be reported. They concern principally about the defect density appearing in a Kerr-like nonlinear optical medium [36, 40, 41]. The state below the bifurcation threshold is a homogeneous state (so we will deal with a primary bifurcation). The state after the threshold is a hexagonal pattern. We also compare the results for two effective viscosities. Finally, we compare the systems in the discussion and conclusions section.

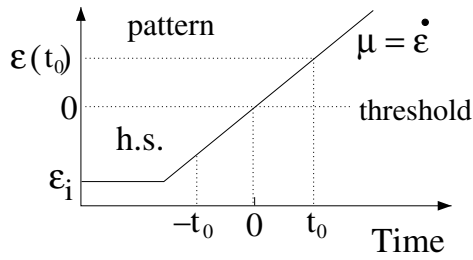


**Fig. 2.** Sketch of the measurement process in this kind of experiments (h.s. stands for homogeneous state, and the interval  $[-t_0, t_0]$  corresponds to the critical slowing down).

## 2 Measurement process

All results shown in this article follow a measurement process which can be explained by the next steps: The system is set in a homogeneous stationary state below the symmetry-breaking bifurcation ( $\epsilon_i < 0$ ). In that state, the control parameter is linearly increased with a rate of change  $\mu$ . When the control parameter reaches the value  $\epsilon(t_0) > 0$ , the structure abruptly gets formed, and then a snapshot of the pattern is taken to analyze it. It is crucial that the increase of the control parameter through all the experiment would be linear.

In order to obtain the number of defects in the emerging structure, we have use different methods, depending on the kind of image and dimensionality of the order parameter. In figure 3 can be seen the patterns obtained in the four experimental systems studied. As it can be seen, there is a pattern of stripes, a pattern of square symmetry and two patterns of hexagonal type.

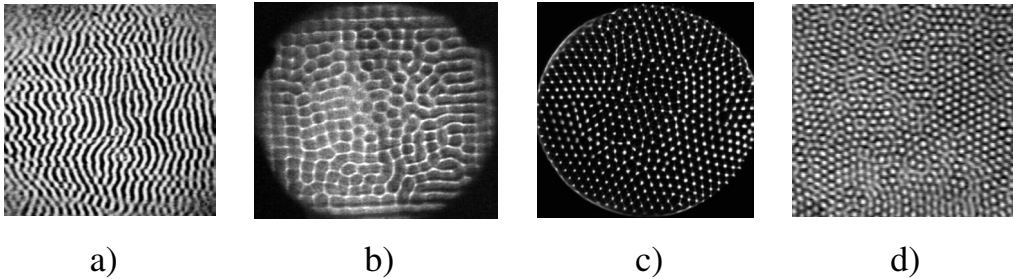


**Fig. 3.** Patterns appearing after the threshold in the systems presented in this article. (a) Kerr-like optical system with translation (non-locality) (b) Rayleigh–Bénard convection pattern (c) Bénard–Marangoni convection pattern (d) Kerr-like optical system without translation.

The pattern of stripes it is very easily analyzed: defects correspond to dislocations in the stripes structure. They can be counted either by visual inspection or by complex demodulation of the Fourier peak corresponding to the stripes. The phase singularities correspond to zeros of the amplitude in the complex demodulated image.

In the case of a square pattern, the analysis of the number of defects is much more complicated in general, due to the two kind of defects that could be observed, that is to say: dislocations of either modes and the grain boundaries dividing regions with different global orientation. This would make the complex demodulation technique very difficult unless the orientation of the two modes would be anchored. That was what was made. In this way it is possible to complex demodulate two more or less wide peaks at an angle of  $\pi/2$ .

The analysis for the case of hexagonal symmetry pattern happens to be equally complicated than the case of coexisting domains of squares with various global orientations. It is difficult, in this case, to anchor the structure at one global direction without also removing the other kind of defects. Then, what had been done is to use the Voronoi analysis [37, 42]. This analysis builds for each lattice site its Voronoi cell, which allows to extract all the connectivity information of the structure. By means of this data it is possible to infer the most common topological defects of hexagonal structures (penta-hepta), and obtain the exponents for the number of defects

upon the rate of increase of the control parameter. Another good possibility is to isolate one or few defects (corresponding to only one domain of global orientation) in order to check their evolution backwards by complex demodulation [38]. The exponents obtained in a three modes pattern experiment by counting pentagons, heptagons or polygons different than hexagons are consistent. among them.

The Voronoi analysis in a square symmetry pattern is not possible due to a geometric instability of the coordination number [6].

### 3 Hydrodynamical systems

We restrict ourselves into the study of thermoconvective systems, heated from below in a homogeneous way. They were first considered by Bénard [43]. We consider the temperature difference between the top and the bottom of the liquid layer as the experimental control parameter  $\Delta T$ . For low values of  $\Delta T$  the heat transport is only done efficiently by conduction. Therefore it will be attained a linear temperature profile upon the depth  $\zeta$ ,

$$T(z) = T_0 + \Delta T \frac{\zeta}{h}, \quad (17)$$

where  $h$  is the depth of the fluid layer and  $T_0$  the temperature of the bottom ( $\zeta = 0$ ).

This temperature profile influences on the density stratification of the fluid, which can be modelled in a first approximation by:

$$\rho(T) = \rho_0 (1 - \alpha \Delta T), \quad (18)$$

where  $\alpha$  is the volumetric thermal expansion coefficient. Although there is also a variation of other parameters due to the temperature profile, it is assumed that the variation is small and does not influences on the dynamical regimes of the systems. Along with this, if the stratification is considered only in the gradient of hydrostatic pressure term, the Boussinesq approximation is used in interpreting the results.

The density stratification tries to destabilize the conductive state when fluctuations exist, due to the Archimedes buoyancy force. The destabilizing effect of buoyancy can be offset owing to the stabilizing effects of thermal diffusion and viscous dissipation, i.e.: if the time needed for the volume which fluctuates to move an infinitesimal is longer than the time needed by the stabilizing forces to counteract the fluctuation. The buoyancy time is defined as:

$$\tau_b = \sqrt{\frac{h}{g\alpha\Delta T}}, \quad (19)$$

where  $g$  is the acceleration of gravity. The stabilizing effects are governed by the following characteristic times:

$$\tau_\theta = \frac{h^2}{\kappa}, \quad \tau_\nu = \frac{h^2}{\nu}, \quad (20)$$

where  $\kappa$  and  $\nu$  are the thermal diffusivity and the kinematical viscosity, respectively.  $\tau_\theta$  is the typical time of stabilization of the temperature by conduction in a liquid layer of depth  $h$ .

Classically, the conduction convection bifurcation in a Rayleigh–Bénard system (a system where the surface tension effects are neglected, as it can occur, for example, if the top of the liquid layer is bounded by a solid surface) is parameterized by the Rayleigh number  $Ra$  [44]:

$$Ra = \frac{\tau_\theta \tau_\nu}{\tau_b^2}. \quad (21)$$

In this way, if the Rayleigh number is greater than a critical value ( $Ra_c$ ), the bifurcation is crossed over. Therefore it is possible to define the control parameter  $\epsilon$  as:

$$\epsilon \equiv \frac{Ra - Ra_c}{Ra_c} = \frac{\Delta T - \Delta T_c}{\Delta T_c}. \quad (22)$$

For  $\epsilon \approx 0$ , any small enough fluctuation will evolve (decay or grow) exponentially in time with a typical response time inversely proportional to  $\epsilon$ . The correlation length scales with a critical exponent 0.5 [45].

When, the system is upper bounded by a fluid state, as in the case of a system open to the atmosphere, it is needed also to take into account the interface tension effects. This kind of convection is called Bénard–Marangoni convection. This introduces a new non-dimensional number called the Marangoni number  $Ma$ ,

$$Ma = \frac{\tau_\theta \tau_\nu}{\tau_\sigma^2}, \quad (23)$$

where:

$$\tau_\sigma = \sqrt{\frac{h^3 \rho_0}{\left| \frac{\partial \sigma}{\partial T} \right| \Delta T}}, \quad (24)$$

and  $\rho_0$  is the density at the mean temperature and  $\sigma$  is the surface tension. The main effect of this change on the relevant behavior at the threshold is the kind of pattern selected and the predominant characteristic time. When both effects (buoyancy and surface tension) are important the system at threshold verifies the Nield equation [46]. It is important to our discussion to consider that the Bénard–Marangoni convection is slightly subcritical. Therefore, rigorously, expression 8 does not apply near the threshold enough.

The experimental set-up used in this systems has been extensively used in the past by the Complex Systems Group. A sketch of it and a detailed description could be found in [37, 38] regarding the Bénard–Marangoni system and in [6, 39] for the Rayleigh–Bénard case. In all cases, the used fluids were Silicone oils of different nominal viscosities. The main difference regarding the measurements is due to the high sensitivity of the fluid layer to any temperature sensor you put nearby, if the experiment is open to the atmosphere. Therefore, the measurements in Bénard–Marangoni had been made after a learning step, where for each ramp of the control parameter, the temperature of the liquid surface was measured in the moment of the appearance of the structure, in order to know the reduced control parameter value, when the dynamics is restored. The range of possible time quenches for both experiments is limited by the system thermal inertia and the initial value of the reduced control parameter (fast quenches) and the slow dynamics characteristic time due to inhomogeneities in the system (slow quenches).

All the experimental results confirm a scaling law for the density of defects upon the rate of increase of the control parameter. However, the exponents are diverse.

In summary, if we plot the exponent appearing in the power law for the density of defects (equation (16)) (figure 4), we can see that the exponent is the one expected for a mean-field system (1/2), for the case of Rayleigh–Bénard. This is the case of having less than three modes in the state. Also the experiment has been done at the lowest viscosity of the fluid (20 cSt). One can see that the exponent decreases as the number of modes does and the viscosity does.

## 4 Optical systems

We will restrict ourselves to a Kerr-like non-linear optical system. It consists of a liquid crystal light valve (LCLV) in which impinges a spatially uniform laser beam. This LCLV is inserted in a feedback loop. For an extensive review see Residori [41]. The LCLV is made of a liquid crystal layer (which is highly birefringent and consequently phase modulating) and of a photoconductive layer (which is sensitive to the light intensity), and of a mirror sandwiched by the other two layers. The boundaries are treated in such a way we have a planar geometry, that is: in absence of applied field the director vector field of the liquid crystal remains parallel to the boundaries of the LCLV. On one hand, if an electric field perpendicular to the boundaries is applied there is a critical value for which the liquid crystal molecules turn over to follow the field. On the other hand, the incident light to the photoconductive layer diminishes locally its impedance making the effective electric field higher and consequently more efficiently rotates the molecules. Different orientations of the molecules in different places of the LCLV, makes

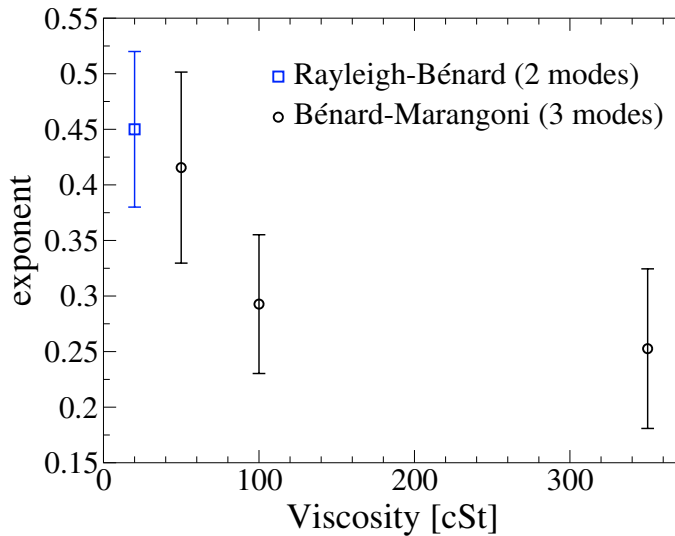


**Fig. 4.** Exponents for the number of defects upon viscosity in the convection experiments. The exponents for the case of Bénard–Marangoni (circles) have been considered as those which fulfill at least one of the counting methods (see text, section 2).

that the light reflecting on the mirror would be spatially phase modulated. The recently read state, in the form of a modulated wavefront is carried by a fiber bundle, which carries coherently the information through a point to point mapping. Afterwards, the wavefront is let to a free propagation length which converts the phase modulation into an amplitude modulation (Talbot effect). This intensity modulation writes a new state to the photoconductive layer. If the phase to amplitude conversion only comes from the Talbot effect, this is a purely diffractive set-up. Thus, this feedback allows the optical system to be a Kerr-like one. The phase of the wavefront evolves following the equation:

$$\frac{\partial \phi(x, y, t)}{\partial t} = -\frac{\phi(x, y, t) - \phi_0}{\tau} + D \nabla_{\perp}^2 \phi(x, y, t) + \alpha I_{fb}(x, y, t), \quad (25)$$

where  $\tau$  is the local relaxation time,  $D$  is the diffusive constant of the medium and  $\phi_0$  the working point set by the applied voltage  $V_0$  when light does not arrive to the photoconductive layer.  $I_{fb}$  is the light that impinges to that layer, and  $\alpha$  phenomenologically determines the effect of the layer to the phase change through the voltage variation. The sign of  $\alpha$  defines whether the Kerr-like medium is focusing or de-focusing. The feedback light intensity comes from the free propagation of the field outgoing from the Kerr medium  $E_0 e^{i\phi(x, y, t)}$ ; within the paraxial approximation at a distance  $L$  of free propagating beam,

$$E(x, y, L, t) = e^{\frac{i\lambda L}{4\pi} \nabla_{\perp}^2} E(x, y, 0, t), \quad (26)$$

which is the electric field defining, in principle, the intensity of feedback. The sign of  $\alpha$  can be changed, at a first approximation, making the free-propagation length negative. If the feedback includes some non-locality (as a rotation, or a translation, among other possibilities, of the fiber bundle) this should appear in equation (25) changing the feedback term to for example  $I_{fb}(x + \Delta x, y, t)$  in the case of a translation in the  $x$  direction.

The experimental set-up used in this systems has been extensively used in the past by the Istituto Nazionale di Ottica Applicata. A sketch of it and a detailed description could be found in [36] regarding the system with a translation inserted in the feedback loop and in [39] concerning the case of the three modes LCLV system. Moreover, an extensive description of variations on the experimental set-up can be found in [41] and references therein.

The main differences between both experiments are the existence of such non locality and the values for the free propagation length (3.5 cm/–6 cm respectively). The translation breaks the symmetry of the spontaneous hexagonal symmetry giving rise to standing stripes with a non zero group velocity along the direction of the translation. This group velocity sweeps away

the phase singularities which appear in the system, and this had to be taken into account when measuring the density of defects, due to the perfect appearance of stripes on the lateral boundary through coherent transport. In this kind of systems, the measurements are limited on the hand of fast quenches by the LCLV inertia and, on the hand of slow quenches, by the characteristic time of drifting defects either due to the translation or to small inhomogeneities in the system.

In the case of the translation of the feedback loop, it is found that the number of defects follows a power law (once the shrinking effective area has been taken into account) and that the exponent agrees with a mean field theory ( $\rho \sim \mu^{0.5 \pm 0.04}$ ) [36].

In the system where there appear three modes, there is not the relatively high motion of defects due to the group velocity of the structure, so it is not necessary to take into account a shrinking area. Nevertheless, small inhomogeneities in the system set a limit for slow quenches, too. In this case, we made the experiment for two working points (corresponding to an applied a.c. voltage, which determines the response time of the LCLV under external illumination): 4.18 V at 2.16 kHz and 6.53 V at 1.94 kHz. Under these conditions, comparing the response of the LCLV, it was measured that  $\tau_r(4.18 \text{ V}) = 2.11 \cdot \tau_r(6.53 \text{ V})$ . The main measurements were obtained making linear ramps of the control parameter (light input intensity) and taking a snapshot of the pattern at the time the dynamics was restored. That image was analyzed by means of Voronoi analysis. The obtained curves for the density of defects upon the quench time rescaled by the relative response time are shown in figure 5.

In figure 5 it can be seen two distinguished domains separated by  $\ln(\tau_r^* \mu) \approx -0.5$ . The solid (dashed) line is a power law adjusted to the 6.53 V (4.18 V) case for points at the left (right) region. The other solid (dashed) line is a power law with the same exponent as obtained before adjusted to the case of 4.18 V (6.53 V) for points at the left (right) region showing good agreement of the adjustment in the regions and cases where the number of points are too few.

Therefore we can conclude that in this kind of experimental systems there are two distinguished regions consistent with power laws. The exponent is for the case of small (large) rates of increase of the order parameter  $0.15 \pm 0.01$  ( $0.28 \pm 0.04$ ). Neither of them follows a mean-field theory. They are of the order of those obtained by high viscosity Bénard–Marangoni systems.

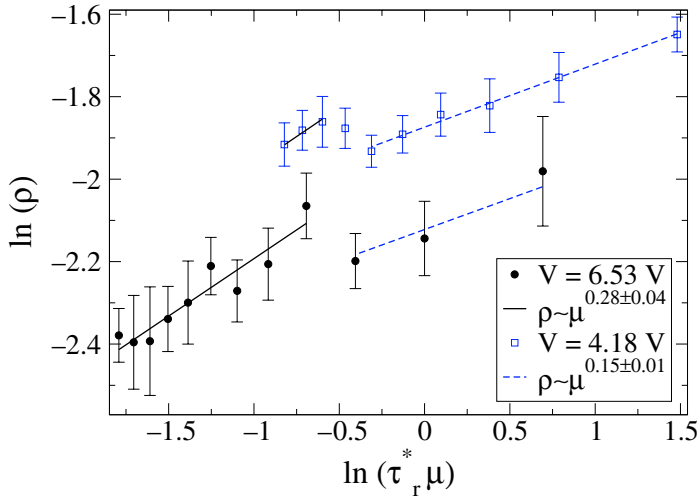


**Fig. 5.** Density of defects upon the rescaled rate of increase of the control parameter in logarithmic scale. The rescaling parameter  $\tau_r^*$  is 1 s for the 6.53 V case and  $\tau_r(4.18 \text{ V})/\tau_r(6.53 \text{ V}) \text{ s} = 2.11 \text{ s}$  for the 4.18 V case. See the text for the meaning of the adjusted power laws.

## 5 Discussion and conclusions

It has been proved that it is possible to extend the mechanism of Kibble–Zurek to bifurcations of out-of-equilibrium systems in continuum media. Regarding the specific experiments reported here we found the scaling laws predicted by the above mechanism, at least over a range of rate of increase of the control parameter through the threshold of primary bifurcations.

A priori, one of the main drawbacks of the mechanism reported here is that it is not always applicable in the case of having a subcritical bifurcation (equivalent to a first order phase transition). However, if the subcriticality is smaller than  $|\epsilon(-t_0)|$  the fluctuations which determine the density of defects already survive till well after the bifurcation. Thus, the subcriticality only sets a limit for the slow quenches ( $\mu$  small enough).

The translation in the feedback loop leads to the reduction of defects by coherent transport. Moreover, as this feedback is introduced in a non local way, the system fall into a mean field system. Consequently, this kind of system verifies  $\rho \sim \sqrt{\mu}$ .

Regarding to the Rayleigh–Bénard system, the experiments confirm that there could be bifurcations leading to more than one mode pattern which verify not only the Kibble–Zurek mechanism, but the corresponding exponents of a mean field theory, accordingly with the steady scaling exponents [45].

In summary, the deviations from the mean field only occur in systems where there are more than two interacting modes (in the studied cases, three), without the global orientation fixed. This disagreement is not due to the possibility in this kind of states of appearance of other types of defects (for example: boundary grains) which are not zero dimensional ones, because they follow the same scaling relation, thus not modifying the results.

Thermal effects do not have to do very much in this discrepancy, since the thermal fluctuations are negligible unless the system is very near a thermodynamic critical point [11]; which is not our case.

It is possible to think that the measurements using the Voronoi analysis could not be complete, because there are other zero dimensional defects which are not (at the time of taking the snapshot) penta-hepta, although once the dynamics is restored they evolve to penta-hepta [38]. The fact that other defects exist which are not detected as penta-hepta and which are less stable (consequently, the faster is the quench, the larger is their number) could explain partially that in this case the exponent measured is lower than expected. On the other hand, at a greater viscosity, these kind of defects should tend to the penta-hepta at lower rates, thus this effect is more remarkable. However, the Voronoi analysis was made not only for penta-hepta, but for sites with coordination number different to six, giving the same results.

As open question, this disagreement could be explained for the low correlation among defects in different modes, though this critical exponent ( $\nu$ ) is the same that those for the correlation length. Nevertheless, the exponent  $z\nu$  is the one corresponding to only one mode. In conclusion, the correlation in such a system should be weaker than in a mean field theory, so the system could be considered as having a high aspect ratio, or being spatially extended. That correlation will diminish also for increasing viscosities. All this effects come from having a multi-component order parameter, where different components interact non-linearly, but with small correlations.

In addition to the Kibble–Zurek mechanism, there could exist others that made the scaling laws would not hold over the whole range of increase rates, as can be seen in the results of the three modes LCLV system. The explanation of such behavior could rely on the elastic effects related to the oscillations of the liquid crystal molecules around their new equilibrium position parallel to the electric field. Another possibility is that the behavior would be related to some oscillations found in some numerical simulations [47]. This is an interesting issue, because this oscillations are predicted to occur in time. The question on how this oscillations imply the appearance of two regimes in the system it is open yet.

Finally, this kind of experiments could be an indirect determination of the steady critical exponents, which are much more difficult to measure directly [48].

The authors acknowledge W. Zurek and R. Ribotta for useful discussions. SC and WGV wish to thank F.T. Arecchi for his hospitality during the research about optical systems. Work was partly supported by the Spanish MCyT Contract No. BFM2002-02011, by PIUNA, by the Italy-Spain Integrated Action HI97-30 and by ESF COSLAB. S.C. acknowledges financial support from the “Asociación de Amigos de la Universidad de Navarra”.

We wish specially dedicate this article to the memory of Carlos Pérez-García with whom we have had very fruitful, and sometimes encouraging discussions on defects, pattern formation and the frontiers in Science.

## References

1. D.R. Nelson, B.I. Halperin, *Phys. Rev. B* **19**, 2457 (1979)
2. T.W.B. Kibble, *J. Phys. A* **9**, 1387 (1976)
3. W.H. Zurek, *Phys. Rep.* **276**, 177 (1996)
4. A. Joets, R. Ribotta, *J. Statis. Phys.* **64**, 981 (1991)
5. R. Ribotta, A. Belaidi, A. Joets, *Singularities, Defects and Chaos in Organized Fluids, in Geometry and Topology of Caustics – Caustics '02*, edited by I. of Mathematics, Polish Academy of Sciences (2004), pp. 223–238
6. S. Casado, W. González-Viñas, H. Mancini, *Phys. Rev. E* **74**, 047101 (2006)
7. G. Toulouse M. Kléman, *J. Phys. Lett.* **37**, 149 (1976)
8. M. Kléman, *Points, Lignes, Parois* (Éditions de Physique, Orsay, 1977)
9. N.D. Mermin, *Rev. Mod. Phys.* **51** (1979)
10. L. Michel, *Rev. Mod. Phys.* **52**, 617 (1980)
11. M.C. Cross, P.C. Hohenberg, *Rev. Mod. Phys.* **65**, 851 (1993)
12. P. Hohenberg, J. Swift, *Phys. Rev. A* **46**, 4773 (1992)
13. W.H. Zurek, *Nature* **317**, 505 (1985)
14. M.V. Berry, *Singularities in Waves and Rays, in Physique des Défauts*, edited by R. Balian, M. Kléman, J.P. Poirier (North-Holland, 1981), École d'Été de Physique Théorique, Session XXXV, pp. 453–543
15. W.H. Zurek, U. Dorner, P. Zoller, *Phys. Rev. Lett.* **95**, 105701 (2005)
16. D.I. Uzunov, *Introduction to the Theory of Critical Phenomena* (World Scientific, Singapore, 1993)
17. P. Couillet, L. Gil, J. Lega, *Phys. Rev. Lett.* **62**, 1619 (1989)
18. A. Rajantie, *Int. J. Mod. Phys. A* **17**, 1 (2002)
19. A. Rajantie, *Contemp. Phys.* **44**, 485 (2003)
20. I. Chuang, R. Dürer, N. Turok, B. Yurke, *Science* **251**, 1336 (1991)
21. M.J. Bowick, L. Chandar, E.A. Schiff, A.M. Srivastava, *Science* **263**, 943 (1994)
22. S. Digal, R. Ray, A.M. Srivastava, *Phys. Rev. Lett.* **83**, 5030 (1999)
23. P.C. Hendry, N.S. Lawson, R.A.M. Lee, P.V.E. McClintock, C.D.H. Williams, *Nature* **368**, 315 (1994)
24. C. Bäuerle, Y.M. Bunkov, S.N. Fischer, H. Godfron, G.R. Pickett, *Nature* **382**, 332 (1996)
25. V.M. Ruutu, V.B. Eltsov, A.J. Gill, T.W.B. Kibble, M. Krusius, Y.G. Makhlin, B. Placais, G.E. Volovik, W. Xu, *Nature* **382**, 334 (1996)
26. V.M. Ruutu, V.B. Eltsov, M. Krusius, Y.G. Makhlin, B. Placais, G.E. Volovik, *Phys. Rev. Lett.* **80**, 1465 (1998)
27. V.B. Eltsov, T.W.B. Kibble, M. Krusius, V.M.H. Ruutu, G.E. Volovik, *Phys. Rev. Lett.* **85**, 4739 (2000)
28. Y. Bunkov, *Physica B* **329**, 70 (2003)
29. V.B. Eltsov, M. Krusius, G. Volovik, cond-mat/9809125 v4 (2004)
30. R. Carmi, E. Polturak, *Phys. Rev. B* **60**, 7595 (1999)
31. R. Monaco, R.J. Rivers, E. Kavoussanaki, *J. Low Temp. Phys.* **124**, 85 (2001)
32. R. Monaco, J. Mygind, R.J. Rivers, *Phys. Rev. Lett.* **89**, 080603 (2002)
33. R. Monaco, J. Mygind, R.J. Rivers, *Phys. Rev.* **B67**, 104506 (2003)
34. A. Maniv, E. Polturak, G. Koren, *Phys. Rev. Lett.* **91**, 197001 (2003)
35. R. Monaco, U.L. Olsen, J. Mygind, R.J. Rivers, V.P. Koshelets, *Phys. Rev. Lett.* **96**, 180604 (2006)
36. S. Ducci, P.L. Ramazza, W. González-Viñas, F.T. Arecchi, *Phys. Rev. Lett.* **83**, 5210 (1999)
37. S. Casado, W. González-Viñas, H. Mancini, S. Boccaletti, *Phys. Rev. E* **63**, 057301 (2001)
38. W. González-Viñas, S. Casado, J. Burguete, H. Mancini, S. Boccaletti, *Int. J. Bif. Chaos* **11**, 2887 (2001)
39. S. Casado, Ph.D. thesis (University of Navarra, 2002)
40. F.T. Arecchi, S. Boccaletti, P.L. Ramazza, *Phys. Rep.* **318**, 1 (1999)
41. S. Residori, *Phys. Rep.* **416**, 201 (2005)
42. G. Voronoi, J. Reine, *Angew. Math.* **134**, 198 (1908)
43. H. Bénard, *Rev. Gén. Sci. Pure Appl.* **11**, 1261 (1900)
44. G.I. Barenblatt, *Scaling, Self-Similarity, and Intermediate Asymptotics*, Vol. 14 of *Cambridge Texts in Applied Mathematics* (Cambridge University Press, Cambridge, UK, 1996)
45. J. Wesfreid, P. Bergé, M. Dubois, *Phys. Rev. A* **19**, 1231 (1979)
46. D. Nield, *J. Fluid Mech.* **19**, 341 (1964)
47. E. Moro, G. Lythe, *Phys. Rev. E* **59**, 1303 (1999)
48. V.C. Regnier, G. Lebon, *Q. J. Mech. Appl. Math.* **48**, 57 (1995)